

# Algebraic approach to electro-optic modulation of light: Exactly solvable multimode quantum model

GEORGE P. MIROSHNICHENKO<sup>1</sup>, ALEXEI D. KISELEV<sup>1,\*</sup>, ALEXANDER I. TRIFANOV<sup>1</sup>, AND ARTUR V. GLEIM<sup>1</sup>

<sup>1</sup> Saint Petersburg National Research University of Information Technologies, Mechanics and Optics (ITMO University), Kronverksky Prospekt 49, 197101 Saint Petersburg, Russia

\*Corresponding author: alexei.d.kiselev@gmail.com

Compiled January 15, 2021

We theoretically study electro-optic light modulation based on a quantum model where the linear electro-optic effect and the externally applied microwave field result in the interaction between optical cavity modes. The model assumes that the number of interacting modes is finite and effects of the mode overlapping coefficient on the strength of the intermode interaction can be taken into account through dependence of the coupling coefficient on the mode characteristics. We show that, under certain conditions, the model is exactly solvable and can be analyzed using the technique of the Jordan mappings for the  $su(2)$  Lie algebra. Analytical results are applied to study effects of light modulation on the frequency dependence of the photon counting rate. In contrast to the limiting case of infinitely large number of interacting modes, when the number of interacting modes is finite, the sideband intensities reveal strongly non-monotonic behavior supplemented with asymmetry of the intensity distribution provided the pumped mode is not central. We also analyze different regimes of two-modulator transmission and establish the conditions of validity of the semiclassical approximation by applying the methods of polynomially deformed Lie algebras for analysis of the model with quantized microwave field. © 2021 Optical Society of America

**OCIS codes:** (230.4140) Modulators; (270.4180) Multiphoton processes; (270.5290) Photon counting; (270.5565) Quantum communications; (190.4975) Parametric processes;

<http://dx.doi.org/10.1364/ao.XX.XXXXXX>

## 1. INTRODUCTION

The quantum information science being a new rapidly developing branch of the modern informatics that analyzes how quantum systems may be used to store, transmit and process information heavily relies on quantum optical information technologies where units of information are represented by photons [1]. Quantum optics is at the heart of quantum communication methods such as quantum cryptography, quantum teleportation, and dense coding [2–6].

Quantum photonics and the optical information technology provide opportunities for manipulating the properties of single photons and using them in many fields [7–11]. For instance, quantum encoding of information underlies a variety of practical schemes developed for quantum cryptography. These include the schemes based on polarization [12–14] and phase [15, 16] coding, implementations of quantum cryptography that use entangled photons [17–20] and quantum cryptography protocols based on continuous variables [21, 22].

Electro-optical modulators are key devices for proper oper-

ation of the above schemes of quantum information processing. These devices have also been used in quantum information methods to monitor and control different photon quantum states [16, 23–28].

In solid-state and soft condensed matter physics, there is a wealth of electro-optic effects [29–35] that underlie the mode of operation of a number of optical devices such as modulators, tunable spectral filters, polarizing converters and optical switches. The linear electro-optic effect (the Pockels effect) that occurs in noncentrosymmetric nonlinear crystals such as lithium niobate ( $\text{LiNbO}_3$ ) crystals will be of our primary interest. Though the classical physics of this effect is well understood [29, 30], the current and emerging applications of the modulators in the field of quantum information and processing systems necessitate developing quantum approaches to frequency and phase modulation [36, 37].

A consistent quantum theory of phase modulation requires the quantum description of the phase. The problems related to the quantum phase operator and phase measurements have an

almost century long history dating back to the original paper by Dirac [38] and have been the subject of intense studies (a collection of important papers can be found, e.g., in [39]). In particular, the quantum theory of phase and instantaneous frequency along with the interferometry methods of measurements are described in Refs. [36, 37]. In these studies, quantization of spectrally limited optical fields was performed by identifying a slowly varying envelope of the creation operator and limiting its spectrum to a narrow band around the carrier frequency.

A quantum scattering theory based black-box approach to electro-optic modulators is developed in Refs. [40, 41]. In this method, the modulators are regarded as the scattering devices producing a multimode output from a single-mode input.

An alternative approach to phase modulation elaborated in early studies [30, 42] uses the method of coupled classical modes of radiation field (the classical wave coupling theory of the electro-optic effect is also discussed in Refs [43, 44]). According to this approach, phase modulation of laser radiation results from the interaction of cavity eigenmodes caused by time periodic modulation of the dielectric constant of the nonlinear crystal placed in the resonator. In Ref. [45], a quantum theory of the electro-optic phase modulator is formulated in terms of the Hamiltonian describing the intermode interaction in the subspace of single photon states.

The common feature of the theoretical considerations presented in [40, 41, 45] is that the number of modes is assumed to be infinitely large whereas the strength of interaction (the coupling coefficient) between the modes is independent of the mode characteristics. Though these assumptions greatly simplify theoretical analysis, they introduce the difficulties related to the unitarity of the scattering matrix [40, 41] and are inapplicable to the case where the modulator is based on ultra-high quality whispering gallery mode microresonators made out of electro-optically active materials [46–49].

Such resonators are characterized by the non-equidistant spectrum of the eigenmodes, so that only a small number of modes are involved in the interaction induced by the externally applied microwave field. The case of three interacting modes was theoretically studied in Refs. [47, 50–52]. An important result of these studies is that dependence of the intensity of sidebands on the power of the microwave pump shows the saturation effect which cannot be explained by the models where the number of interacting modes is indefinitely large.

In this paper our goal is to examine the case bridging the gap between the above mentioned models of electro-optic modulators. For this purpose, we formulate an exactly solvable model in terms of the Hamiltonian describing the parametric process where the number of interacting optical modes is finite and the strength of interaction varies depending on the mode characteristics such as the mode number related to the mode frequency. Owing to algebraic properties of this model, theoretical analysis can be performed using the generalized Jordan mapping technique and the results can be further extended with the help of the mathematical methods developed in [53].

An important point is that, within our approach, the modulator is explicitly treated as a multiport device (multiport beam splitter) that may produce and manipulate multiphoton states. Such devices are known to be promising for a variety of applications [54]. In particular, the modulator generated multiphoton states are used as carriers of information in the frequency-coded [15, 23, 55] and subcarrier multiplexing [56] quantum key distribution systems.

The paper is organized as follows.

In Sec. 2, we introduce our model and show that the mode number dependence of the coupling coefficient can be reasonably modeled so as to generate the theory where the algebraic structure of the multimode operators is represented by the generators of the  $su(2)$  Lie algebra. In the semiclassical approximation where the microwave is assumed to be a classical field, analytical expressions for the evolution operator and the quasienergy spectrum are obtained in Subsection 2.B. In Subsection 3.A, we apply the theoretical results to study the effect of light modulation on the photon counting rate and present the results of numerical analysis. The limiting case where the number of interacting modes increases indefinitely (the large  $S$  limit) is studied in Subsection 3.B. The theory is applied to analyze different regimes of two-modulator transmission in Subsection 3.C. Finally, in Sec. 4, we draw the results together and make some concluding remarks. Details on the Jordarn mapping technique are relegated to Appendix A. In Appendix B, we show how the method of polynomially deformed algebras can be applied to study the quantum model with quantized microwave field and derive the applicability conditions for the semiclassical approximation.

## 2. MODEL

As an electro-optical modulator we consider a nonlinear crystal of the length  $L$  placed between the metal electrodes parallel to the direction of propagation (the  $z$  axis). Radio frequency wave (microwave) excited between the electrodes propagates through the crystal along the  $z$  axis. The microwave mode is characterized by the wavenumber  $k_{MW} = 2\pi/L$  and the frequency  $\Omega_{MW} = k_{MW}v_{MW}$ , where  $v_{MW}$  is the phase velocity of the mode.

As is illustrated in Fig. 1, the crystal can be regarded as the reflectionless electro-optic cavity (resonator) and we assume that all the traveling optical modes are subject to the periodic boundary conditions. Then the longitudinal wavenumber (the  $z$  component of the wave vector) of the modes takes the quantized values:

$$k_m = \frac{2\pi m}{L}, \quad m \in \mathbb{Z}. \quad (1)$$

The frequency of the central (carrier) optical mode which is typically excited by the laser pulse is given by

$$\omega_{\text{opt}} = |k_{\text{opt}}|v_{\text{opt}} = \Omega|m_{\text{opt}}|, \quad \Omega = \frac{2\pi}{L}v_{\text{opt}}, \quad (2)$$

where  $k_{\text{opt}} = \frac{2\pi m_{\text{opt}}}{L}$ ,  $v_{\text{opt}}$  is the phase velocity of light in the ambient dielectric medium and  $m_{\text{opt}}$  stands for the mode number of this operational optical mode. Note that the magnitude of the optical mode number  $m_{\text{opt}}$  is typically of the order  $10^4 - 10^6$  and, owing to mismatch between the phase velocities  $v_{MW}$  and  $v_{\text{opt}}$  the frequency of the microwave mode may generally differ from  $\Omega$ ,  $\Omega_{MW} = \Omega v_{MW}/v_{\text{opt}} \neq \Omega$ .

In classical optics, the well-known picture suggests that, owing to the linear electro-optic effect in the nonlinear crystal, the externally applied microwave field modulates the phase of the optical wave producing a multimode output observed as the multiple sidebands that a single optical carrier develops after modulation [29, 30]. The modulation process thus involves interaction of different optical modes mediated by the microwave field and the traveling modes appear to be coupled.

The strength of the microwave-field-induced intermode coupling is mainly determined by the two factors: (a) the electro-optic coefficient and (b) the overlapping coefficients represented

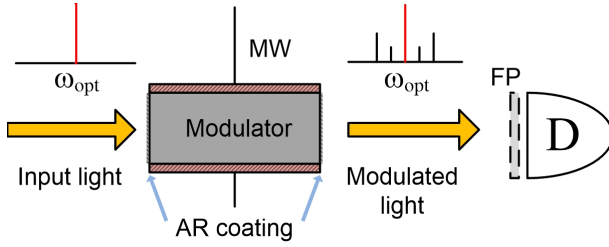


**Fig. 1.** Modulated light emerging after the modulator driven by the microwave field (MW) passes through a Fabry-Perot filter (FP) and is collected by a photodetector (D). Anti-reflective (AR) coating is applied to both faces of the electro-optic cavity.

by the averages of a product of the spatial distributions of the modes and the microwave field over the volume of interaction. These factors may severely constrain the number of efficiently interacting modes. For instance, in Refs. [23, 47, 50–52], theoretical considerations of electro-optic modulation are based on the quantum models with three interacting optical modes. Our model can be regarded as a generalization of these results.

The electro-optically induced interactions generally falls within the realms of the parametric processes in nonlinear quantum systems and the theoretical technique developed in early studies on this subject [42, 57–60] can be invoked to model them. Our starting point is the Hamiltonian of the photons written in the following form:

$$H/\hbar = \Omega_{\text{MW}} b^\dagger b + \Omega A_0 + \frac{\gamma_0}{f_{\text{max}}} \{A_+ b + A_- b^\dagger\}, \quad (3)$$

$$A_0 = \sum_m m a_m^\dagger a_m, \quad A_- = \sum_m f(m) a_m^\dagger a_{m+1}, \quad A_+ = A_-^\dagger, \quad (4)$$

where a dagger will denote Hermitian conjugation,  $b^\dagger$  ( $b$ ) is the creation (annihilation) operator of the photons in the microwave mode,  $a_m^\dagger$  ( $a_m$ ) is the creation (annihilation) operator of the optical photons numbered by the mode number  $m$ ,  $\gamma_0$  is the bare intermode coupling constant (interaction parameter) and  $f(m)/f_{\text{max}}$  is the normalized function describing the mode number dependence of the intermode interaction strength,  $f_{\text{max}} = \max_m f(m)$ . Note that in our notations the polarization index has been dropped. It implies that all the modes are assumed to be linearly polarized along a principal axis of the crystal and we shall restrict our considerations to the geometry where the state of polarization remains intact.

### A. Hamiltonian and $su(2)$ algebra

Formula (3) presents the Hamiltonian with the three-boson interaction written in the rotating wave approximation. This approximation assumes that the intermode interaction is dominated by the quasis resonant terms that commute with the operator of the linear momentum:  $K/\hbar = k_{\text{MW}} b^\dagger b + \sum_m k_m a_m^\dagger a_m$  and are slowly varying in the representation of interaction (they are proportional to  $\exp(\pm i[\Omega - \Omega_{\text{MW}}]t)$ ), whereas the non-resonant terms are of minor importance. They produce negligibly small effects and hence can be disregarded.

Another key assumption taken in our model is that the intensity of the microwave mode is sufficiently high for its quantum properties to be ignored. So, it can be described as the classical wavefield. In this semiclassical approximation, the creation (annihilation) operator  $b$  ( $b^\dagger$ ) is replaced with the c-number amplitude  $B \exp[-i\Omega_{\text{MW}}t]$  ( $B^* \exp[i\Omega_{\text{MW}}t] \equiv |B| \exp[i(\Omega_{\text{MW}}t + \phi)]$ ),

where an asterisk will indicate complex conjugation and  $\phi$  is the phase of the amplitude  $B^*$ , and the Hamiltonian (3) can be recast into the form:

$$H/\hbar = \Omega A_0 + \frac{\gamma}{f_{\text{max}}} \left\{ A_+ \exp[-i(\Omega_{\text{MW}}t + \phi)] + A_- \exp[i(\Omega_{\text{MW}}t + \phi)] \right\}, \quad (5)$$

where  $\gamma = \gamma_0 |B|$ . Applicability of the semiclassical approach is discussed in Appendix B where the method of polynomially deformed algebras developed in Ref. [53] is used to analyze the model with quantized microwave mode.

From the above discussion, the number of interacting modes is finite and the mode number range for these modes can generally be defined by the inequality of the form:

$$m_{\text{min}} < m \leq m_{\text{max}}, \quad (6)$$

where  $m_{\text{min}}$  and  $m_{\text{max}}$  are both the positive integers. The optical central (operational) mode (2) is in the middle of the interval (6) with the mode number given by

$$m_{\text{opt}} = \frac{m_{\text{max}} + m_{\text{min}} + 1}{2} \quad (7)$$

and we assume that the most efficient intermode coupling occurs in the vicinity of  $m_{\text{opt}}$ , whereas the strength of interaction decays to the limit of non-interacting modes at the boundaries of the interaction interval (6). Such behavior can be modeled through the function

$$f(m) = \sqrt{(m - m_{\text{min}})(m_{\text{max}} - m)} \quad (8)$$

describing dependence of the intermode coupling on the mode number.

The interacting modes can be conveniently relabeled by the shifted mode number  $\mu$  as follows

$$m = m_{\text{opt}} + \mu, \quad -S \leq \mu \leq S, \quad S = \frac{m_{\text{max}} - m_{\text{min}} - 1}{2}, \quad (9)$$

$$a_{m_{\text{opt}} + \mu} \equiv a_\mu, \quad a_{m_{\text{opt}} + \mu}^\dagger \equiv a_\mu^\dagger, \quad (10)$$

where  $2S + 1 = m_{\text{max}} - m_{\text{min}} = 2f_{\text{max}}$  is the number of interacting modes.

The operators that enter the Hamiltonian (5) of our model can now be written in the following form

$$A_0 = m_{\text{opt}} N + J_0, \quad N = \sum_{\mu=-S}^S a_\mu^\dagger a_\mu, \quad J_0 = \sum_{\mu=-S}^S \mu a_\mu^\dagger a_\mu, \quad (11)$$

$$A_- \equiv J_- = \sum_{\mu=-S}^{S-1} \sqrt{(S + \mu + 1)(S - \mu)} a_\mu^\dagger a_{\mu+1}, \quad (12)$$

$$A_+ \equiv J_+ = J_-^\dagger = \sum_{\mu=-S}^{S-1} \sqrt{(S + \mu + 1)(S - \mu)} a_{\mu+1}^\dagger a_\mu, \quad (13)$$

where  $N$  is the total photon number operator. The important point is that the operators  $J_0$  and  $J_\pm$  given in Eqs. (12) and (13) meet the well-known commutation relations for the generators of the  $su(2)$  Lie algebra:

$$[J_0, J_\pm] = \pm J_\pm, \quad [J_+, J_-] = 2J_0. \quad (14)$$

Note that the operator of total photon number  $N$  and the Casimir operator given by

$$J^2 = J_0^2 + (J_+ J_- + J_- J_+)/2 = J_x^2 + J_y^2 + J_z^2, \quad (15)$$

$$J_z \equiv J_0, \quad J_\pm = J_x \pm iJ_y \quad (16)$$

both commute with the generators of  $su(2)$  algebra.

Mathematically, the technique of the generalized Jordan mappings for bosons [61] can be applied to derive the relations (14). This technique is briefly reviewed in Appendix A.

The operators (11)–(13) can now be substituted into Eq. (5) with  $f_{\max} = (2S + 1)/2$  to yield the resulting expression for the time-dependent Hamiltonian of our semiclassical model

$$H(t)/\hbar = \omega_{\text{opt}}N + \Omega J_z + \frac{2\gamma}{2S+1} \left\{ J_+ \exp[-i(\Omega_{\text{MW}}t + \phi)] + J_- \exp[i(\Omega_{\text{MW}}t + \phi)] \right\}. \quad (17)$$

## B. Operator of evolution and quasienergy spectrum

Now we show how the algebraic structure of the model can be used to evaluate the operator of evolution and the quasienergy spectrum of the time-periodic Hamiltonian (17):  $H(t + T_{\text{MW}}) = H(t)$ , where  $T_{\text{MW}} = 2\pi/\Omega_{\text{MW}}$  is the period of the microwave mode.

The operator of evolution (propagator) can be found by solving the initial value problem:

$$i\hbar \frac{d}{dt} U(t) = H(t)U(t), \quad U(0) = I, \quad (18)$$

where  $I$  is the identity operator. In the Floquet representation, the propagator takes the form of a product:

$$U(t) = U_P(t) \exp(-iQt/\hbar), \quad (19)$$

where  $U_P(t + T_{\text{MW}}) = U_P(t)$  is the time-periodic operator and  $Q$  is the quasienergy operator. In our case, equation (19) can be regarded as the rotating wave ansatz

$$U(t) = U_P(t)U_R(t) \quad (20)$$

with the unitary operator

$$U_P(t) = \exp[-i(m_{\text{opt}}N + J_z)\Omega_{\text{MW}}t] \quad (21)$$

performing the transformation to the “rotating coordinate system” and the quasienergy operator is given by

$$Q/\hbar = m_{\text{opt}}\omega N + \omega J_z + \frac{2\gamma}{2S+1} \left\{ J_+ \exp(-i\phi) + J_- \exp(i\phi) \right\}, \quad \omega = \Omega - \Omega_{\text{MW}}. \quad (22)$$

The rotation operator

$$R(\phi, \beta) = \exp(-i\phi J_z) \exp(-i\beta J_y) \quad (23)$$

can now be used to transform the quasienergy operator into the diagonal form

$$Q_d/\hbar = R^\dagger(\phi, \beta)QR(\phi, \beta) = m_{\text{opt}}\omega N + \Gamma J_z, \quad (24)$$

$$\omega + i \frac{4\gamma}{2S+1} = \Gamma \exp[i\beta], \quad \Gamma = \sqrt{\omega^2 + [4\gamma/(2S+1)]^2}, \quad (25)$$

so that the Fock states  $|n_{-S}, \dots, n_\mu, \dots, n_S\rangle$  characterized by the mode occupation numbers are the eigenstates of the quasienergy operator (24) with the quasienergies given by

$$E(n, m_z)/\hbar = n m_{\text{opt}}\omega + m_z \Gamma, \quad (26)$$

where  $n = \sum_{\mu=-S}^S n_\mu$  is the total number of photons and  $m_z = \sum_{\mu=-S}^S \mu n_\mu$  is the azimuthal quantum number,  $-nS \leq m_z \leq nS$ . Note that a set of the Fock states characterized by the quantum

numbers  $n$  and  $m_z$  forms a vector space  $\mathcal{F}_{n, m_z}$  which can further be divided into subspaces  $\mathcal{F}_{n, m_z}^j$  classified by the eigenvalues of the Casimir operator (15):  $J^2|n, j, m_z, \kappa\rangle = j(j+1)|n, j, m_z, \zeta\rangle$ , where  $|m_z| \leq j \leq nS$  is the angular momentum number and  $\zeta$  is the integer enumerating the basis eigenstates of  $\mathcal{F}_{n, m_z}^j$ ,  $\kappa \in \{1, \dots, \dim \mathcal{F}_{n, m_z}^j\}$ . In other words, the space  $\mathcal{F}_{n, m_z}$  can generally be decomposed into the direct sum of subspaces  $\mathcal{F}_{n, m_z}^j$ :  $\mathcal{F}_{n, m_z} = \bigoplus_j \mathcal{F}_{n, m_z}^j$ . For example, at  $S = 1$ , it can be shown that  $0 \leq j = n - 2k \leq n$  with  $k \in \{0, 1, \dots\}$  and all the subspaces  $\mathcal{F}_{n, m_z}^j$  are one-dimensional,  $\dim \mathcal{F}_{n, m_z}^j = 1$ . Given the total photon number  $n$ , the dimension of the space  $\mathcal{F}_n = \bigoplus_{m_z} \mathcal{F}_{n, m_z}$  is known to be  $\dim \mathcal{F}_n = (n+2S)!/(2S)!n!$  and, at  $S > 1$ , the subspaces  $\mathcal{F}_{n, m_z}^j$  are not necessarily one-dimensional.

Equations (21)–(24) can now be substituted into the Floquet representation (19) to yield the operator of evolution in the final form:

$$U(t) = e^{-i\Omega_{\text{MW}}tJ_z} R(\phi, \beta) e^{-iTtJ_z} R^\dagger(\phi, \beta) e^{-i\omega_{\text{opt}}tN}. \quad (27)$$

Using this formula in combination with the identity for the rotation of the annihilation operator (A9) derived in Appendix A, we can describe the temporal evolution of the photon annihilation operator  $a_\mu$  as follows

$$a_\mu(T) = U^\dagger(T) a_\mu U(T) = \sum_{\nu=-S}^S M_{\mu\nu} a_\nu, \quad (28)$$

$$M_{\mu\nu} = e^{-i(\omega_{\text{opt}} + \mu\Omega_{\text{MW}})T} e^{-i(\mu-\nu)\phi} U_{\mu\nu}^S(T), \quad (29)$$

$$U_{\mu\nu}^S(T) = \sum_{\mu'=-S}^S d_{\mu\mu'}^S(\beta) d_{\nu\mu'}^S(\beta) e^{-i\mu'TT} = (-1)^\nu e^{-i(\mu+\nu)\tilde{\alpha}} d_{\mu\nu}^S(\tilde{\beta}), \quad (30)$$

where  $T$  is the duration of intermode interaction which is the time an optical wavefield takes to propagate through the electro-optic modulator and the expression for  $U_{\mu\nu}^S(T)$  is simplified by using the addition formula for the Wigner  $D$  functions [62],  $D_{\mu\nu}^S(\alpha, \beta, \gamma) = \exp[-i\mu\alpha] d_{\mu\nu}^S(\beta) \exp[-i\nu\gamma]$ , with the angles  $\tilde{\alpha}$  and  $\tilde{\beta}$  defined through the following relations:

$$2\tilde{\alpha} = \pi + \arg\{\sin^2\beta + (1 + \cos^2\beta) \cos(\Gamma T) + 2i \cos\beta \sin(\Gamma T)\}, \quad (31a)$$

$$\cos\tilde{\beta} = \cos^2\beta + \sin^2\beta \cos(\Gamma T), \quad (31b)$$

$$\sin\tilde{\beta} = \sin\beta [\cos\tilde{\alpha} \cos\beta (1 - \cos(\Gamma T)) - \sin\tilde{\alpha} \sin(\Gamma T)]. \quad (31c)$$

Details on derivation of these relations are relegated to Appendix A.

## 3. RESULTS

The model described in the previous section represents the electro-optic modulator as a multiport device that may generally be used to manipulate multimode photonic states. Quantum dynamics of such states involves different frequency modes and lie at the heart of applications based on frequency encoding [16, 23, 28] and quantum effects dealing with the frequency entangled photons [27, 63]. For these applications and effects an important first step is to study the effect of light modulation on the photon counting rate.

For this purpose, in this section, we use the analytical results of Sec. 2 to evaluate the counting rate as the one-electron

photodetection probability per unit time. We find that it can be written in the factorized form with the modulation form-factor expressed in terms of the matrix (30) and present a number of numerical results for this form-factor. We also discuss what happen in the limiting case where the number of interacting modes increases indefinitely and  $S \rightarrow \infty$  (the large  $S$  limit) and apply the theory to the problem of two-modulator transmission.

### A. Photon counting rate

The cavity modes of the modulator are excited by the photons with the carrier frequency  $\omega_{\text{opt}}$  that propagate through the electro-optic device. Owing to the electro-optic effect, the traveling microwave field inside the cavity gives rise to the inter-mode interaction. For the modes initially prepared in the state described by the density matrix of the radiation field  $\rho_F(0)$ , at the instant of time  $T$ , the density matrix is given by

$$\rho_F(T) = U(T)\rho_F(0)U^\dagger(T), \quad (32)$$

where  $U(t)$  is the operator of evolution (27) (the losses are neglected). Note that, similar to Eq. (28),  $T$  is the duration of interaction (the time it takes for a light wave to travel through the region where electro-optic modulation occurs) and Eq. (32) assumes the lossless dynamics of the density matrix  $\rho_F$ .

An important characteristics of the radiation field is the averaged photon number of the mode with the mode number  $\mu$ :

$$\langle N_\mu \rangle(T) = \text{Tr}_F\{a_\mu^\dagger a_\mu \rho_F(T)\} = \text{Tr}_p\{a_\mu^\dagger(T) a_\mu(T) \rho_F(0)\}. \quad (33)$$

We can now use the relation (28) to derive the explicit expression for the average (33):

$$\langle N_\mu \rangle(T) = \sum_{\nu', \nu=-S}^S U_{\mu\nu'}^S(T) U_{\mu\nu}^S(T) e^{i(\nu-\nu')\phi} \langle a_{\nu'}^\dagger a_\nu \rangle(0) \quad (34)$$

where  $\langle a_{\nu'}^\dagger a_\nu \rangle(0) = \text{Tr}_F\{a_{\nu'}^\dagger a_\nu \rho_F(0)\}$ . For the special case of single mode pumping where the optical mode with the mode number  $\nu$  is the only mode initially excited in the resonator and  $\langle a_{\nu'}^\dagger a_\nu \rangle(0) = \delta_{\nu\nu'} \langle N_\nu \rangle(0)$ , we have

$$\langle N_\mu \rangle(T) \equiv \langle N_\mu \rangle = |U_{\mu\nu}^S(T)|^2 \langle N_\nu \rangle(0). \quad (35)$$

Typically, this is the central mode which is excited and  $\nu = 0$ .

We consider an experimental setup depicted in Fig. 1. In such a setup, the output of the electro-optic modulator is connected to a Fabry-Perot filter via the optical fiber channel. Then the light wave passed through the filter is collected by a photodetector with sufficiently wide bandwidth.

The wavefield at the exit of the modulator is characterized by the density matrix  $\rho_F(T)$  given in Eq. (32). An important point is that the modes of the output light field should be matched to the modes of the optical fiber. In what follows we shall assume that they are perfectly correlated (see, e.g., Chapter 1.4 in the book [64]). So, in the interaction picture, the electric field operator,  $\mathbf{E}(\mathbf{r}, t)$ , of light normally incident on the filter can be decomposed into its positive and negative frequency parts,  $\mathbf{E}_+(\mathbf{r}, t)$  and  $\mathbf{E}_-(\mathbf{r}, t)$ , as follows

$$\begin{aligned} \mathbf{E}(\mathbf{r}, t) &= \mathbf{E}_+(\mathbf{r}, t) + \mathbf{E}_-(\mathbf{r}, t), \\ \mathbf{E}_+(\mathbf{r}, t) &= \mathbf{E}_+^\dagger(\mathbf{r}, t) = \sum_{\mu=-S}^S \mathbf{E}_\mu^{(+)}(\mathbf{r}) a_\mu(t), \end{aligned} \quad (36)$$

where  $a_\mu(t) = a_\mu(T) \exp[-i\omega_\mu(t - T)]$ ,  $a_\mu(T)$  is given in Eq. (28),  $\omega_\mu = \omega_{\text{opt}} + \mu\Omega$  is the mode frequency and  $\mathbf{E}_\mu^{(+)}(\mathbf{r})$  is

the complex valued vector amplitude that generally depends on a number of characteristics of the mode such as the wavevector, the frequency and the state of polarization. Throughout this paper we have used notations where the index describing the state of polarization of the modes is suppressed by assuming that all the modes are linearly polarized along the unit vector  $\hat{\mathbf{e}}$ , so that  $\mathbf{E}_\mu^{(+)}(\mathbf{r}) = E_\mu^{(+)}(\mathbf{r})\hat{\mathbf{e}}$ .

For the light transmitted through the filter,  $\mathbf{E}_f = \mathbf{E}_+^{(f)} + \mathbf{E}_-^{(f)}$ , we have

$$\mathbf{E}_+^{(f)}(\mathbf{r}, t) = \sum_{\mu=-S}^S \tilde{\mathbf{E}}_\mu^{(+)}(\mathbf{r}) a_\mu(t), \quad \tilde{\mathbf{E}}_\mu^{(+)}(\mathbf{r}) = \mathbf{T}_f(\omega_f, \omega_\mu) \mathbf{E}_\mu^{(+)}(\mathbf{r}), \quad (37)$$

where  $\mathbf{T}_f(\omega_f, \omega_\mu)$  is the transmission matrix of the filter and  $\omega_f$  is the filter frequency. The filter is also characterized by the bandwidth  $\Delta\omega_f$ , so that the filter transmission is negligibly small provided that  $|\omega_f - \omega_\mu| > \Delta\omega_f$ .

We now briefly discuss the process of photoelectric detection of the light transmitted through the filter based on the model of an idealized photodetector described in the monograph [65] (Chapter 14). Our task is to compute the photon counting rate as the one-electron photodetection probability per unit time. For this purpose, we take the assumption of a narrowband optically isotropic filter with  $\Delta\omega_f < \Omega$  and  $\mathbf{T}_f(\omega_f, \omega_\mu) = T_f(\omega_f, \omega_\mu) \mathbf{I}_3$ , where  $\mathbf{I}_3$  is the  $3 \times 3$  identity matrix. So, the result can now be obtained by using the quasi-monochromatic approximation (see Chapter 14.2.2 in the book [65]). For an atom located at  $\mathbf{r} = \mathbf{r}_0$ , the energy of interaction between the atom and the radiation field in the dipole approximation is

$$V = -(\mathbf{d} \cdot \mathbf{E}_f(\mathbf{r}_0)), \quad (38)$$

where  $\mathbf{d}$  is the operator of the electric dipole moment.

We can now closely follow the line of reasoning presented in Ref. [65] and obtain the one-electron detection probability rate

$$p(\omega_f) = \sum_{\mu=-S}^S |T_f(\omega_f, \omega_\mu)|^2 \langle N_\mu \rangle K(\omega_\mu) \quad (39)$$

expressed in terms of the frequency response function of the photodetector

$$\begin{aligned} K(\omega_\mu) &= H(\omega_\mu - \omega_g) \int \sigma(\omega_\mu - \omega_g, \kappa) g(\omega_\mu - \omega_g, \kappa) \\ &\quad \times |\langle \omega_\mu - \omega_g, \kappa | (\mathbf{d} \cdot \hat{\mathbf{e}}) | G \rangle E_\mu^{(+)}(\mathbf{r}_0)|^2 d\kappa, \end{aligned} \quad (40)$$

where  $H(x)$  is the Heaviside unit step function,  $|G\rangle$  is the ground (bounded) state of the atom with the negative energy equal to  $-\hbar\omega_g$  (it is the eigenstate of the Hamiltonian of the atomic system  $H_A$ :  $H_A|G\rangle = -\hbar\omega_g|G\rangle$ ),  $|\omega_e, \kappa\rangle$  is the excited free electron (unbound) state characterized by the positive energy  $\hbar\omega_e$  ( $H_A|\omega_e, \kappa\rangle = \hbar\omega_e|\omega_e, \kappa\rangle$ ) and possibly by other variables represented by  $\kappa$ ;  $\sigma(\omega_e, \kappa)$  is the density of the excited states and  $g(\omega_e, \kappa)$  is the probability for the electron in the state  $|\omega_e, \kappa\rangle$  to be collected and registered by the detector.

For the broadband detector with  $K(\omega_\mu) \approx K(\omega_{\text{opt}})$ , the expression for the counting rate (39) can be further simplified

giving the result in the factorized form:

$$\begin{aligned} p(\omega_f) &\approx p_0(\omega_{\text{opt}})p_{\text{mod}}(\omega_f, T), \\ p_0(\omega_{\text{opt}}) &= K(\omega_{\text{opt}})\langle N_\nu \rangle(0), \end{aligned} \quad (41)$$

$$\begin{aligned} p_{\text{mod}}(\omega_f, T) &= \sum_{\mu=-S}^S |T_f(\omega_f, \omega_\mu)U_{\mu\nu}^S(T)|^2, \\ |U_{\mu\nu}^S(T)|^2 &= |d_{\mu\nu}^S(\tilde{\beta})|^2, \end{aligned} \quad (42)$$

where we have used formulas (35) and (30) for the averaged photon number  $\langle N_\mu \rangle$  and  $U_{\mu\nu}^S(T)$ , respectively. From Eqs. (41) and (42), it is clear that the photon count form-factor  $p_{\text{mod}}(\omega_f, T)$  accounts for the combined effect of the modulator and the filter, whereas the factor  $p_0(\omega_{\text{opt}})$  gives the counting rate without filtering and modulation. The form-factor  $p_{\text{mod}}(\omega_f, T)$  thus might be called the light modulation form-factor of the photon count rate.

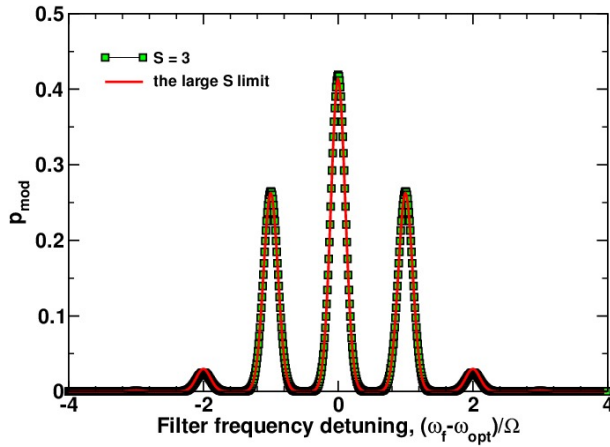


**Fig. 2.** (Color online) The photon counting rate form-factor  $p_{\text{mod}}$  as a function of the filter frequency detuning computed from Eq. (42) at the intermode coupling parameter  $\gamma/\Omega = 0.1$  (the regime of weak intermode coupling). The other parameters are:  $T_{\text{max}}^{(f)} = 1$  is the maximal transmittance of the filter;  $\sigma_f/\Omega = 0.15$  is the bandwidth of the filter;  $T = 2\pi/\Omega$  is the time of intermode interaction and  $\omega/\Omega = (\Omega - \Omega_{\text{MW}})/\Omega = 0.01$ .

In our calculations, the frequency dependence of the filter transmittance is modeled by the Gaussian shaped curve

$$|T_f(\omega_f, \omega)|^2 = T_{\text{max}}^{(f)} \exp[-(\omega_f - \omega)^2/\sigma_f^2], \quad (43)$$

where  $\sqrt{\ln 2}\sigma_f$  is the Gaussian half width at half maximum that determines the bandwidth of the filter  $\Delta\omega_f = \sigma_f$  and  $T_{\text{max}}^{(f)}$  is the maximal transmittance of the filter at the peak  $\omega_f = \omega$ . Figures 2–6 show the photon count light modulation form-factor  $p_{\text{mod}}(\omega_f, T)$  computed from Eq. (42) either as a function of the dimensionless filter frequency detuning  $(\omega_f - \omega_{\text{opt}})/\Omega$  (Figs. 2–4) or in relation to the intermode coupling parameter  $\gamma/\Omega$  (Figs. 5 and 6). In these figures, the mode initially excited in the electro-optic cavity is central with  $\nu = 0$  and the parameters are:  $T_{\text{max}}^{(f)} = 1$ ,  $\sigma_f/\Omega = 0.15$ ,  $\omega/\Omega = 0.01$  and  $T = 2\pi/\Omega$ .

### B. Regime of large number of interacting modes: the large $S$ limit

In our model, the operator of evolution (27) describing the effect of electro-optically induced light modulation is represented by

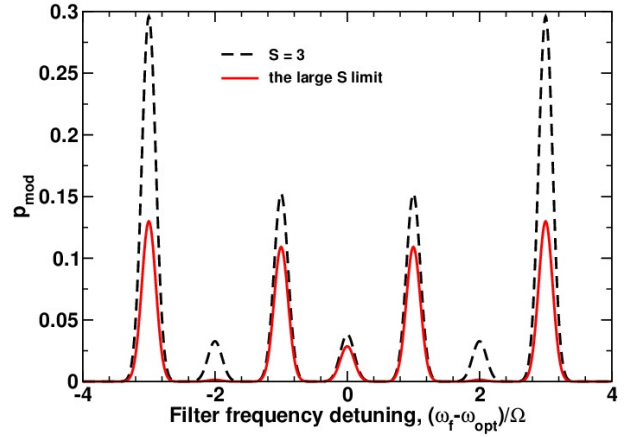


**Fig. 3.** (Color online) The photon counting rate form-factor  $p_{\text{mod}}$  as a function of the filter frequency detuning at the intermode coupling parameter  $\gamma/\Omega = 0.4$  (the regime of intermediate intermode coupling). Other parameters are listed in the caption of Fig. 2.

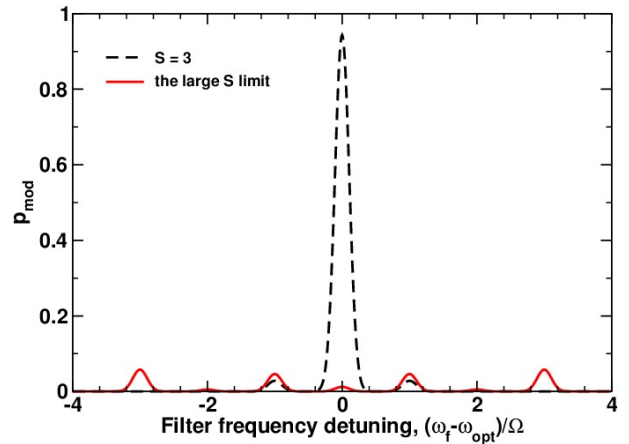


**Fig. 4.** (Color online) The photon counting rate form-factor  $p_{\text{mod}}$  as a function of the filter frequency detuning at the intermode coupling parameter  $\gamma/\Omega = 0.9$  (the regime of strong intermode coupling). Other parameters are listed in the caption of Fig. 2.

the matrix  $U_{\mu\nu}^S(T)$  given by Eq. (30). The latter is the  $(2S+1) \times (2S+1)$  matrix, where  $2S+1$  is the number of interacting modes. In this section, we discuss the limiting case where the number of interacting modes is large and  $S \rightarrow \infty$ .

From Eq. (30), the elements of the matrix  $U_{\mu\nu}^S(T)$  are determined by the Wigner  $D$  functions  $D_{\mu\nu}^S(\tilde{\alpha}, \tilde{\beta}, \tilde{\alpha} + \pi)$  with relations for the angles  $\tilde{\alpha}$  and  $\tilde{\beta}$  given by Eq. (31). Equation (25) can be used in combination with the relations (31) to derive the large  $S$  asymptotics for the angles

$$\sin \beta \sim \frac{2\gamma}{|\omega|} S^{-1}, \quad (44a)$$

$$\tilde{\alpha} \xrightarrow{S \rightarrow \infty} \frac{\pi + \omega T}{2}, \quad \omega = \Omega - \Omega_{\text{MW}}, \quad (44b)$$

$$\tilde{\beta} \sim -\frac{g}{S}, \quad g = \frac{4\gamma}{|\omega|} \sin(|\omega|T/2). \quad (44c)$$

Our next step starts with the well-known expression for the

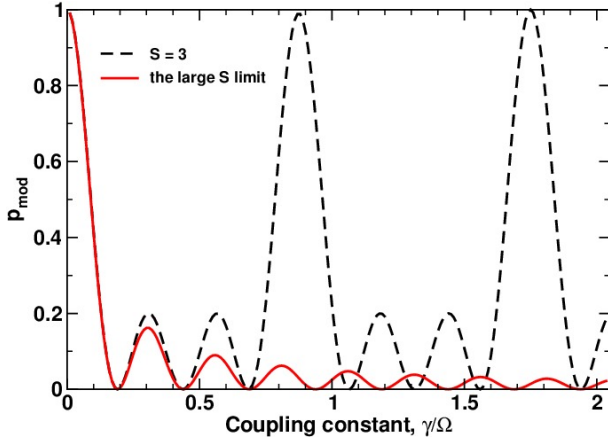


**Fig. 5.** (Color online) The photon counting rate form-factor  $p_{\text{mod}}$  as a function of the coupling parameter  $\gamma/\Omega$  at  $\omega_f = \omega_{\text{opt}}$ . Other parameters are listed in the caption of Fig. 2.

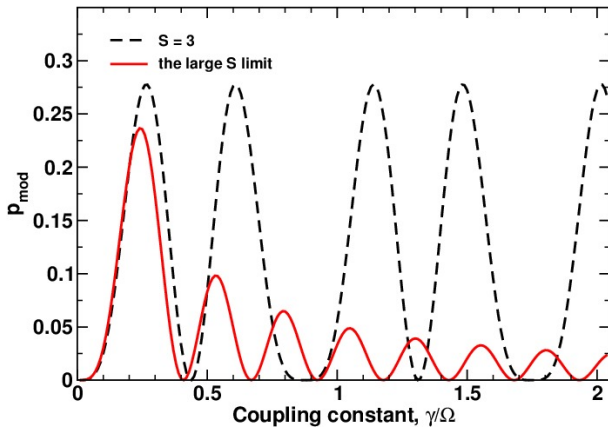


**Fig. 6.** (Color online) The photon counting rate form-factor  $p_{\text{mod}}$  as a function of the coupling parameter  $\gamma/\Omega$  at  $\omega_f = \omega_2 = \omega_{\text{opt}} + 2\Omega$ . Other parameters are listed in the caption of Fig. 2.

Wigner  $d$ -functions [61]

$$d_{\mu\nu}^S(\tilde{\beta}) = \sqrt{\frac{(S+\nu)!(S-\nu)!}{(S+\mu)!(S-\mu)!}} \sin^{\nu-\mu}\left(\frac{\tilde{\beta}}{2}\right) \times \cos^{\nu+\mu}\left(\frac{\tilde{\beta}}{2}\right) P_{S-\nu}^{(\nu-\mu, \nu+\mu)}(\cos \tilde{\beta}), \quad (45)$$

where  $P_n^{(\alpha, \beta)}(x)$  denotes the Jacobi polynomial [66], and uses asymptotics of the Jacobi polynomials given by the Mehler-Heine formula [67]:

$$\lim_{n \rightarrow \infty} n^{-\alpha} P_n^{(\alpha, \beta)}(\cos(z/n)) = \lim_{n \rightarrow \infty} n^{-\alpha} P_n^{(\alpha, \beta)}(1 - z^2 n^{-2}/2) = \left[\frac{z}{2}\right]^{-\alpha} J_\alpha(z), \quad (46)$$

where  $J_\alpha(z)$  is the Bessel function of the first kind [66] (outside this subsection symbols  $J_\mu$  without arguments denote the generators of  $su(2)$ ).

From Eqs. (44)–(46), it is rather straightforward to find that the asymptotic behavior of the Wigner  $d$  functions and the matrix

$U_{\mu\nu}^S$  is given by

$$d_{\mu\nu}^S(\tilde{\beta}) \xrightarrow{S \rightarrow \infty} J_{\mu-\nu}(g), \quad (47)$$

$$U_{\mu\nu}^S(T) \xrightarrow{S \rightarrow \infty} (-i)^{\mu-\nu} e^{-i(\mu-\nu)\omega T/2} J_{\mu-\nu}(g) e^{-i\nu\omega T}. \quad (48)$$

Now we apply the asymptotic relation (48) to describe, in the large  $S$  limit, the effect of electro-optic modulation on temporal evolution of light after passing through the modulator at  $t > T$ . From Eq. (36), the averaged positive frequency part of the electric field can be written as follows

$$\langle \mathbf{E}_+(\mathbf{r}, t) \rangle = \sum_{\mu=-S}^S \mathbf{E}_\mu^{(+)}(\mathbf{r}) e^{-i\omega_\mu(t-T)} \langle a_\mu(T) \rangle_0, \quad (49)$$

where  $\omega_\mu = \omega_{\text{opt}} + \mu\Omega$  and  $\langle a_\mu(T) \rangle_0 \equiv \text{Tr}_F\{a_\mu(T)\rho_F(0)\}$ .

$$\begin{aligned} \langle \mathbf{E}_+(\mathbf{r}, t) \rangle &\xrightarrow{S \rightarrow \infty} \sum_{\mu, \nu} \mathbf{E}_\mu^{(+)}(\mathbf{r}) e^{-i(\mu-\nu)(\Omega t - \psi)} J_{\mu-\nu}(g) e^{-i\omega_\nu t} \langle a_\nu \rangle_0 \\ &\approx \sum_{\mu, \nu} e^{-i(\mu-\nu)(\Omega t - \psi)} J_{\mu-\nu}(g) \mathbf{E}_\nu^{(+)}(\mathbf{r}) e^{-i\omega_\nu t} \langle a_\nu \rangle_0 \\ &= e^{-ig \cos(\Omega t - \psi)} \langle \mathbf{E}_+(\mathbf{r}, t) \rangle_0, \end{aligned} \quad (50)$$

where  $\psi = \omega T/2 - \phi$  and  $\langle \mathbf{E}_+(\mathbf{r}, t) \rangle_0 = \sum_\nu \mathbf{E}_\nu^{(+)}(\mathbf{r}) e^{-i\omega_\nu t} \langle a_\nu \rangle_0$  is the average of the radiation field propagating in the free space without light modulation. The result (50) is obtained with the help of the equality [66]

$$\exp[-ig \cos(\Omega t)] = \sum_{\mu=-\infty}^{\infty} (-i)^\mu e^{-i\mu\Omega t} J_\mu(g) \quad (51)$$

by assuming that the modes are linearly polarized  $\mathbf{E}_\mu^{(+)} = E_\mu^{(+)} \hat{\mathbf{e}}$  and the approximation  $E_\mu^{(+)} \approx E_\nu^{(+)}$  may break only in the region where  $|\mu - \nu|$  is sufficiently large for  $|J_{\mu-\nu}(g)|$  to be negligibly small.

The phase factor  $\exp[-ig \cos(\Omega t - \psi)]$  on the right hand side of Eq. (50) implies that the wave after the modulator becomes phase modulated and  $g$  plays the role of the phase modulation index (the modulation depth). This is the well known result of the simple classical model [30] which in our model is recovered in the large  $S$  limit.

In Figs. 2–4, the filter frequency dependence of the photon count modulation form-factor computed in the large  $S$  limit is compared with  $p_{\text{mod}}$  evaluated at  $S = 3$  (the number of interacting modes equals 7). As is illustrated in Fig. 2, in the case of weak intermode interaction where the coupling constant is small, the differences between the curves are negligible. Referring to Figs. 3 and 4, the latter is no longer the case in the regimes of intermediate and strong coupling.

The effect of electro-optically induced intermode interaction can be clearly seen in Figs. 5 and 6 where the form-factor of the mode with the frequency  $\omega_\mu$  selected by the filter at  $\omega_f = \omega_\mu$  is plotted as a function of the coupling constant  $\gamma$ . For the central mode with  $\mu = 0$ , the results are presented in Fig. 5.

Clearly, in the large  $S$  limit, the coupling constant dependence of  $p_{\text{mod}}$  shown in Fig. 5 demonstrates that the initially pumped mode becomes depleted as the strength of interaction increases, so that the photons spread over the (infinitely) large number of modes. By contrast, the model with  $S = 3$  predicts qualitatively different behavior of the form-factor characterized by oscillations with  $p_{\text{mod}}$  being close to a periodic function of  $\gamma$ .

Mathematically, the oscillating behavior of  $p_{\text{mod}}$  is determined by the elements of the matrix (30) where  $|U_{\mu\nu}^S| = |d_{\mu\nu}^S(\tilde{\beta})|$  is a  $2\pi$  periodic even function of  $\tilde{\beta}$  with  $|d_{\mu\nu}^S(0)| = \delta_{\mu\nu}$  and  $|d_{\mu\nu}^S(\pi)| = \delta_{\mu,-\nu}$ . In addition, from Eq. (31), it can be shown that, given the angle  $\beta$ , the angle  $\tilde{\beta}$  can be regarded as a function of  $\Gamma T$  and  $|\tilde{\beta}(\beta, \Gamma T)| = |\tilde{\beta}(\beta, 2\pi \pm \Gamma T)|$ . This implies that  $|U_{\mu\nu}^S| = |d_{\mu\nu}^S(\tilde{\beta})|$  is a periodic function of  $\Gamma T$ .

From Eq. (25), it can be inferred that, in general, the parameters  $\beta$  and  $\Gamma$  both depend on the coupling constant  $\gamma$ . At  $\gamma \gg |\omega|$ ,  $\beta \approx \pi/2$  and  $\Gamma$  is linearly proportional to  $\gamma$ . So, at sufficiently strong coupling  $|U_{\mu\nu}^S|$  (and thus  $p_{\text{mod}}$ ) will be a periodic function of  $\gamma$ .

In particular, when the phase velocities of microwave and optical fields are matched and  $\omega = \Omega - \Omega_{\text{MW}} = 0$ , we deal with the resonance case where  $\beta = \pi/2$ ,  $\tilde{\alpha} = -\pi/2$  and  $\tilde{\beta} = \Gamma T = 4\gamma T / (2S + 1)$  (see Eq. (A22) in Appendix A). In the large  $S$  limit, it is not difficult to show that  $U_{\mu\nu}^S \rightarrow (-i)^{\mu-\nu} J_{\mu-\nu}(2\gamma T)$  and we obtain the result in the form of Eq. (50) with  $\psi = -\phi$  and  $g = 2\gamma T$ . For finite number of modes, the  $\gamma$  dependence of the photon counting rate is dictated by the coupling dependent factor  $|d_{\mu\nu}^S|^2$ . This factor is an even  $2\pi$  periodic function of the coupling parameter  $4\gamma T / (2S + 1)$ . In contrast, oscillations of the factor  $|J_{\mu-\nu}(2\gamma T)|^2$  rapidly decay in magnitude as  $\gamma$  increases. Figure 6 illustrates that similar effects occur when the detuning  $\omega$  is small and  $\mu = 2$ .

Figures 2–6 present the results obtained by assuming that the mode excited in the cavity is central with  $\nu = 0$ . In this case the model and its large  $S$  limit both predict that  $|U_{\mu,0}^S|^2 = |U_{-\mu,0}^S|^2$  and contributions to the photon counting rate coming from symmetrically arranged sideband modes,  $\mu$  and  $-\mu$ , are equal. This symmetry is evident from the curves shown in Figs. 2–4.

When the pumped mode is not central and  $\nu \neq 0$ , the symmetry between the blue-detuned and red-detuned modes with frequencies  $\omega_\nu + k\Omega$  and  $\omega_\nu - k\Omega$  appears to be broken provided the number of interacting modes is finite. Mathematically, the reason is the difference between the magnitudes of the matrix elements  $|U_{\nu+k,\nu}^S|$  and  $|U_{\nu-k,\nu}^S|$ . By contrast, the symmetry retains in the large  $S$  limit where  $|U_{\nu\pm k,\nu}^S| \rightarrow |J_{\pm k}(g)| = |J_{|k|}(g)k|$ . The results computed at  $\nu = k = 1$  are shown in Fig. 7. They clearly demonstrate pronounced asymmetry between the modes with  $\mu = \nu + 1 = 2$  and  $\mu = \nu - 1 = 0$  that occurs at  $S = 3$ , whereas the curves evaluated in the large  $S$  limit are clearly identical.

### C. Two-modulator transmission

In conclusion of this section we briefly discuss how our results can be extended to the important case where the input state after being transformed by a modulator of a sender (Alice) is transmitted through the optical fiber to a receiver (Bob) that sends the incoming state through of a second modulator. This is a simplified scheme representing the key elements used in frequency-coded setups [15, 23]. We characterize the evolution operator of the system in terms of the matrix  $\mathbf{M}$  [see Eq. (29)] that enter the right hand side of Eq. (28). In our case, this matrix can be written as the product of three matrices

$$\mathbf{M} = \mathbf{M}_2 \mathbf{M}_0 \mathbf{M}_1, \quad (52)$$

$$M_{\mu\nu}^{(0)} = \delta_{\mu\nu} e^{-i\Phi_\mu}, \quad M_{\mu\nu}^{(i)} = e^{-i\Phi_{\mu\nu}^{(i)}} d_{\mu\nu}^S(\beta_i), \quad (53)$$

where the phase shift  $\Phi_\mu = \Phi_0 + \mu\phi_0$  represents the effect of propagation in the optical fiber and the elements of the Alice's (Bob's) modulator matrix,  $\mathbf{M}_1$  ( $\mathbf{M}_2$ ), are expressed in terms

of the phase given by

$$\Phi_{\mu\nu}^{(i)} = \Phi_{00}^{(i)} + \mu(\Omega_{\text{MW}} T_i + \alpha_i + \phi_i) + \nu(\pi + \alpha_i - \phi_i), \quad (54)$$

where  $\Phi_{00}^{(i)} = \omega_{\text{opt}} T_i$ . We assume that the only difference between otherwise identical modulators is the phase of the microwave field,  $\phi_1 = \phi_A$  and  $\phi_2 = \phi_B$ , that plays the role of the tuning parameter. Other parameters of the modulators are:  $T_1 = T_2 = T$ ,  $\alpha_1 = \alpha_2 = \alpha_m$  and  $\beta_1 = \beta_2 = \beta_m$ . Similar to Eq. (30), we can use the relation

$$\sum_{\mu'=-S}^S d_{\mu\mu'}^S(\beta_m) d_{\nu\mu'}^S(\beta_m) e^{-i\mu'\phi_{AB}} = (-1)^\nu e^{-i(\mu+\nu)\tilde{\alpha}} d_{\mu\nu}^S(\tilde{\beta}), \quad (55)$$

$$\phi_{AB} = \phi_A - \phi_B + \Delta, \quad \Delta = \phi_0 + \Omega_{\text{MW}} T + 2\alpha_m \quad (56)$$

to derive the expression for the elements of the matrix (52) in the final form:

$$M_{\mu\nu} = e^{-i\Phi_{\mu\nu}} d_{\mu\nu}^S(\tilde{\beta}), \quad (57)$$

$$\Phi_{\mu\nu} = \psi_0 + \mu(\Omega_{\text{MW}} T + \alpha_m + \tilde{\alpha} + \phi_B) + \nu(\pi + \alpha_m + \tilde{\alpha} - \phi_A), \quad (58)$$

where  $\psi_0 = \Phi_0 + 2\omega_{\text{opt}} T$ . The angles  $\tilde{\alpha}$  and  $\tilde{\beta}$  are determined by Eq. (31) with the set of parameters  $\{\Gamma T, \beta\}$  replaced by  $\{\phi_{AB}, \beta_m\}$ .

In particular, from the suitably modified relation Eq. (31b) it follows that  $\cos \tilde{\beta} = 1$  provided that  $\cos \phi_{AB} = 1$ . At these values of the tuning parameter  $\phi_{AB}$ , the modulators compensate each other and  $M_{\mu\nu} = \delta_{\mu\nu}$ . It implies that, in this regime, for the input light field without sidebands, no sidebands will be detected by Bob's photodetector.

Another limiting case is represented by the regime where the central optical mode is suppressed after passing through Bob's modulator. This regime takes place when the condition

$$d_{00}^S(\tilde{\beta}) \propto P_S(\cos \tilde{\beta}) = 0, \quad (59)$$

where  $P_S(x)$  is the Legendre polynomial, is satisfied.

The intermode coupling should be sufficiently strong,  $\gamma > \gamma_c$ , for the condition (59) to be met. To show this, we note that, the value of  $\cos \tilde{\beta}$  varies from unity to  $\cos(2\beta_m)$  as the phase  $\phi_{AB}$  changes from zero to  $\pi$ . It implies that the condition (59) cannot be fulfilled if the value of  $\cos(2\beta_m)$  is above the largest root of the Legendre polynomial  $P_S$  on the interval between zero and unity:  $[0, 1]$ . By making a simplifying assumption that  $\omega = 0$  ( $\Omega_{\text{MW}} = \Omega$ ) and  $\beta = \pi/2$ , we find that  $\beta_m = \Gamma T$  [ $\Gamma$  is given by Eq. (25)]. Then, for  $T = 2\pi/\Omega$  and  $S = 3$ , the critical coupling ratio  $\gamma_c/\Omega$  can be numerically estimated to be at about 0.0954. Interestingly, when the number of modes increases, the critical coupling ratio approaches the estimate  $\gamma_c/\Omega \approx 0.0957$  obtained from the asymptotic form of the condition (59):  $J_0(2g) = 0$ , where  $g$  is defined in Eq. (44c).

## 4. CONCLUSIONS AND DISCUSSION

In this paper, we have formulated a quantum multimode model of the electro-optic modulator, where the intermode interaction is induced by the microwave field via the linear electro-optic effect (the Pockels effect). This model is shown to be exactly solvable when the strength of coupling between the interacting modes depends on the mode number characterizing its detuning from the central optical mode and the operators [see Eqs. (12)

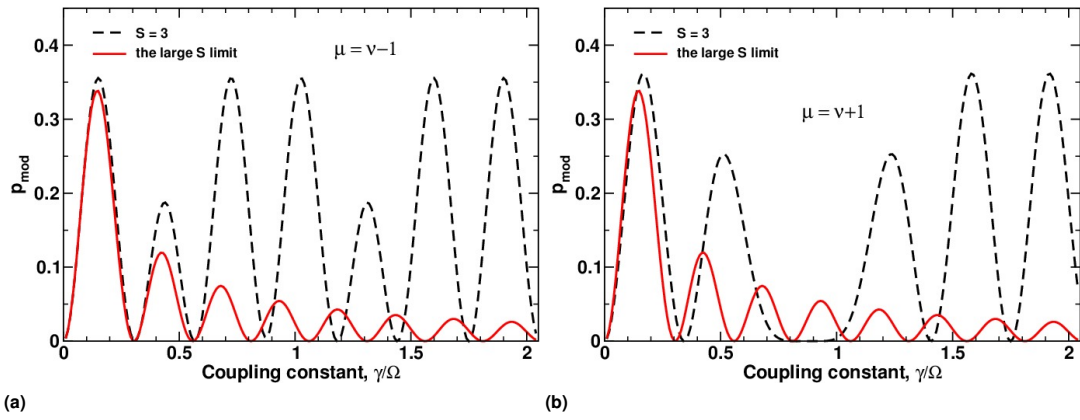


**Fig. 7.** (Color online) The photon counting rate form-factor  $p_{\text{mod}}$  as a function of the coupling parameter  $\gamma/\Omega$  for  $\langle N_\nu \rangle(0) = \delta_{\nu,1} \langle N_1 \rangle(0)$  at (a)  $\omega_f = \omega_0 = \omega_{\text{opt}}$  and (b)  $\omega_f = \omega_2 = \omega_{\text{opt}} + 2\Omega$ .

and (13)] describing the electro-optically induced interaction form the  $su(2)$  Lie algebra with the commutation relations given by Eq. (14).

Within the framework of the semiclassical approach where the microwave field is treated as a classical signal (the validity of this approximation is justified in Appendix B), we have used the analytical expressions for the quasienergy spectrum (26) and the evolution operator (27) in combination with the method of generalized Jordan mappings (see Appendix A) to describe the temporal evolution of the photonic annihilation (creation) operators in terms of the Wigner  $D$  functions [see Eqs. (28)–(31)]. These results are then employed for theoretical investigation into the effects of light modulation on the photon counting rate. Based on the well-known Mandel-Wolf model of an idealized photodetector [65], we have found that the count rate computed as the one-electron photodetection probability per unit time can be written in the factorized form (41) with the light modulation form-factor given by Eq. (42).

Figures 2–7 present the numerical results for the counting rate form-factor evaluated as a function of the frequency and the coupling constant. In particular, the theoretical predictions for the case where  $S = 3$  (the number of interacting modes equals  $2S + 1$ ) are compared with the large  $S$  limit where  $S$  increases indefinitely,  $S \rightarrow \infty$  (this limiting case is discussed in Subsection 3.B). It is found that the differences between these two cases are negligible at small values of the coupling constant (see Fig. 2) and become pronounced as the strength of intermode interaction increases (see Figs. 3–6).

In the large  $S$  limit, coupling constant dependence of the intensities of sidebands shows that the photons spread over available photonic states leading to depletion of the pumped mode (solid lines in Figs. 5–7). This is a consequence of asymptotic behavior in the large  $S$  limit where, similar to the classical optics, the effect of electro-optic light modulation is shown to be determined by the modulating phase factor given by Eq. (51) [see also Eq. (50)].

By contrast, the intensities of sidebands computed as a function of the coupling coefficient at  $S = 3$  (dashed lines in Figs. 5–7) appear to be nearly periodic. Another interesting effect which disappears in the large  $S$  limit can be described as the asymmetry in intensity between the sidebands with the frequencies symmetrically arranged with respect to the pumped mode (e.g. red shifted Stokes and blue shifted anti-Stokes modes). As is illus-

trated in Fig. 7, this asymmetry arises when the pumped mode differs from the central one (the case of detuned pumping).

Analytical results are also employed to describe the two-modulator transmission depending on the microwave phase difference. We have studied the two important limiting regimes where either the modulators compensate each other or have a destructive effect on the central optical mode. The latter is found to occur only if the intermode interaction strength is sufficiently strong and exceeds its critical value.

We now try to place our results into a more general physical context. Generally, an exactly solvable model where the electro-optic modulator is viewed as a multiport device can be employed as a theoretical tool for investigation into numerous effects coming from the complicated quantum dynamics of multimode systems. In addition, this model deals with parametric processes that play important part in the so-called resonator optomechanics [68, 69] representing a new branch of quantum information science that rapidly evolves at the interface of the nanophysics and the quantum theory of light. Making progress in studies of the Casimir effect, new protocols of quantum communication, quantum computing and quantum memory will require further insight into the theory of such parametric processes.

Mathematically, we have demonstrated in Appendix B that it is feasible to apply the methods of polynomially deformed algebras [53] to extend our considerations to the case of quantized microwave field. This case, however, requires a more comprehensive study which is beyond the scope of this paper. On the other hand, our approach provides a useful tool for investigation of high-frequency light modulation in liquid crystal modulators driven by the orientational Kerr effect [32–35]. In particular, the model can be generalized to take into account effects of non-trivial polarization dependent quantum dynamics. This work is now in progress.

We acknowledge partial financial support from the Government of the Russian Federation (Grant No. 074-U01).

## APPENDIX A: JORDAN MAPPING TECHNIQUE

These mappings are defined as follows

$$J_\alpha \mapsto J_\alpha = \sum_{\nu, \mu=-S}^S a_\nu^\dagger J_{\nu\mu}^{(\alpha)} a_\mu \equiv \mathbf{a}^\dagger \mathbf{J}_\alpha \mathbf{a}, \quad (\text{A1})$$

where  $\mathbf{J}_\alpha$  is the  $(2S + 1) \times (2S + 1)$  matrix. The elements  $J_{\nu\mu}^{(\alpha)}$  ( $\equiv [J_\alpha]_{\nu\mu}$ ) of the matrices  $\mathbf{J}_\alpha$  with  $\alpha \in \{0, \pm\}$  are given by

$$J_{\nu\mu}^{(\pm)} = \sqrt{(S \mp \mu)(S \pm \mu + 1)} \delta_{\nu\mu \pm 1}, \quad J_{\nu\mu}^{(0)} = \mu \delta_{\nu\mu}, \quad (\text{A2})$$

where  $\delta_{\nu\mu}$  is the Kronecker symbol. Using the standard bosonic commutation relations

$$[a_\nu, a_\mu^\dagger] = \delta_{\nu\mu}, \quad [a_\nu^\dagger, a_\mu^\dagger] = [a_\nu, a_\mu] = 0 \quad (\text{A3})$$

it is not difficult to check the key useful property of the Jordan construction:

$$[J_\alpha, J_\beta] = \mathbf{a}^\dagger [\mathbf{J}_\alpha, \mathbf{J}_\beta] \mathbf{a}. \quad (\text{A4})$$

The result (14) follows because the matrices  $\mathbf{J}_\pm$  and  $\mathbf{J}_0$  with the elements given in Eq. (A2) satisfy the commutation relations for  $su(2)$  algebra. Another useful relation can be derived for the Baker-Campbell-Hausdorff formula

$$\exp(i\beta J_\alpha) a_\mu \exp(-i\beta J_\alpha) = \sum_{k=0}^{\infty} \frac{i^k \beta^k}{k!} [J_\alpha, a_\mu]_{(k)}, \quad (\text{A5})$$

where  $[J_\alpha, a_\mu]_{(k)}$  stands for the multiple commutator

$$\begin{aligned} [J_\alpha, a_\mu]_{(k)} &= [J_\alpha, [J_\alpha, a_\mu]_{(k-1)}], \\ [J_\alpha, a_\mu]_{(1)} &= [J_\alpha, a_\mu], \quad [J_\alpha, a_\mu]_{(0)} = a_\mu. \end{aligned} \quad (\text{A6})$$

From Eqs. (A1) and (A3) we have

$$[J_\alpha, a_\mu] = - \sum_{\nu=-S}^S J_{\mu\nu}^{(\alpha)} a_\nu, \quad (\text{A7})$$

and formula (A5) can be recast into the final form

$$\exp(i\beta J_\alpha) a_\mu \exp(-i\beta J_\alpha) = \sum_{\nu=-S}^S [\exp(-i\beta J_\alpha)]_{\mu\nu} a_\nu. \quad (\text{A8})$$

An important consequence of Eq. (A8) is the identity

$$\begin{aligned} e^{i\gamma J_z} e^{i\beta J_y} e^{i\alpha J_z} a_\mu e^{-i\alpha J_z} e^{-i\beta J_y} e^{-i\gamma J_z} &= \sum_{\nu=-S}^S [e^{-i\alpha J_z} e^{-i\beta J_y} e^{-i\gamma J_z}]_{\mu\nu} a_\nu \\ &= \sum_{\nu=-S}^S D_{\mu\nu}^S(\alpha, \beta, \gamma) a_\nu \end{aligned} \quad (\text{A9})$$

for the rotated annihilation operator expressed in terms of the Wigner  $D$  functions:  $D_{\mu\nu}^S(\alpha, \beta, \gamma) = \exp[-i\mu\alpha] d_{\mu\nu}^S(\beta) \exp[-i\nu\gamma]$  that, for the irreducible representation of the rotation group with the angular number  $S$ , give the elements of the rotation matrix parametrized by the three Euler angles [61, 62]:  $\alpha$ ,  $\beta$  and  $\gamma$ .

We conclude this section with details on derivation of the expression for the matrix elements of the operator  $\mathbf{U}_S(t)$  given in Eq. (30). This operator can be written in the form

$$\mathbf{U}_S(t) = e^{-i\beta J_y} e^{-i\Gamma J_z} e^{i\beta J_y} = e^{-i\Gamma t(\sin\beta J_x + \cos\beta J_z)}. \quad (\text{A10})$$

More generally, we consider the rotation operator

$$\mathbf{R}(\psi, \hat{\mathbf{m}}) = \exp[-i\psi(\hat{\mathbf{m}} \cdot \mathbf{J})], \quad (\text{A11})$$

where  $\mathbf{J} = (J_x, J_y, J_z)$ ,  $\psi = \Gamma t$  and  $\hat{\mathbf{m}} = (m_x, m_y, m_z) \equiv (m_1, m_2, m_3) = (\sin\beta, 0, \cos\beta)$  is the unit vector directed along

the rotation axis. Equation (A11) defines rotation about the rotation axis  $\hat{\mathbf{m}}$  by the rotation angle  $\psi = \Gamma t$ . Alternatively, this rotation can be parametrized by the Euler angles as follows

$$\mathbf{R}(\psi, \hat{\mathbf{m}}) = \mathbf{R}(\tilde{\alpha}, \tilde{\beta}, \tilde{\gamma}) = e^{-i\tilde{\alpha}J_z} e^{-i\tilde{\beta}J_y} e^{-i\tilde{\gamma}J_z}. \quad (\text{A12})$$

Our task is to express the Euler angles  $\tilde{\alpha}$ ,  $\tilde{\beta}$  and  $\tilde{\gamma}$  in terms of the rotation angle  $\psi = \Gamma t$  and the angle of the rotation axis  $\beta$ . To this end, we begin with the relations

$$\mathbf{R}(\psi, \hat{\mathbf{m}})(\mathbf{n} \cdot \mathbf{J})\mathbf{R}^\dagger(\psi, \hat{\mathbf{m}}) = (\mathbf{R}(\psi, \hat{\mathbf{m}})\mathbf{n} \cdot \mathbf{J}), \quad (\text{A13})$$

$$\mathbf{R}(\tilde{\alpha}, \tilde{\beta}, \tilde{\gamma})(\mathbf{n} \cdot \mathbf{J})\mathbf{R}^\dagger(\tilde{\alpha}, \tilde{\beta}, \tilde{\gamma}) = (\mathbf{R}(\tilde{\alpha}, \tilde{\beta}, \tilde{\gamma})\mathbf{n} \cdot \mathbf{J}), \quad (\text{A14})$$

where  $\mathbf{R}(\psi, \hat{\mathbf{m}})$  and  $\mathbf{R}(\tilde{\alpha}, \tilde{\beta}, \tilde{\gamma})$  are the  $3 \times 3$  rotation matrices, that hold for arbitrary vector  $\mathbf{n}$ .

$$\mathbf{R}(\psi, \hat{\mathbf{m}}) = \mathbf{I}_3 \cos\psi + \hat{\mathbf{m}} \otimes \hat{\mathbf{m}}(1 - \cos\psi) + \mathbf{M} \sin\psi, \quad (\text{A15})$$

where  $\mathbf{I}_3$  is the  $3 \times 3$  identity matrix and  $\mathbf{M}$  is the antisymmetric matrix with the elements  $M_{ij} = -\sum_{k=1}^3 \epsilon_{ijk} m_k$  defined using the unit vector  $\hat{\mathbf{m}}$  and the antisymmetric tensor  $\epsilon_{ijk}$  ( $\epsilon_{123} = 1$ ). In our case, we have

$$\mathbf{M} = \begin{pmatrix} 0 & \cos\beta & 0 \\ \cos\beta & 0 & -\sin\beta \\ 0 & \sin\beta & 0 \end{pmatrix}. \quad (\text{A16})$$

From the other hand, the rotation matrix  $\mathbf{R}(\tilde{\alpha}, \tilde{\beta}, \tilde{\gamma})$  is given by

$$\mathbf{R}(\tilde{\alpha}, \tilde{\beta}, \tilde{\gamma}) = \mathbf{R}_z(\tilde{\alpha})\mathbf{R}_y(\tilde{\beta})\mathbf{R}_z(\tilde{\gamma}) \quad (\text{A17})$$

a product of the rotation matrices of the form:

$$\mathbf{R}_z(\tilde{\alpha}) = \begin{pmatrix} \cos\tilde{\alpha} & -\sin\tilde{\alpha} & 0 \\ \sin\tilde{\alpha} & \cos\tilde{\alpha} & 0 \\ 0 & 0 & 1 \end{pmatrix}, \quad \mathbf{R}_y(\tilde{\beta}) = \begin{pmatrix} \cos\tilde{\beta} & 0 & \sin\tilde{\beta} \\ 0 & 1 & 0 \\ -\sin\tilde{\beta} & 0 & \cos\tilde{\beta} \end{pmatrix}. \quad (\text{A18})$$

The relations linking different parametrizations can now be obtained from the condition:

$$\mathbf{R}(\psi, \hat{\mathbf{m}}) = \mathbf{R}(\tilde{\alpha}, \tilde{\beta}, \tilde{\gamma}) \equiv \mathbf{R}. \quad (\text{A19})$$

Since, for the matrix  $\mathbf{R}(\psi, \hat{\mathbf{m}})$ ,  $R_{13} = R_{31}$ ,  $R_{21} = -R_{12}$  and  $R_{23} = -R_{32}$ , we have

$$\tilde{\gamma} = \tilde{\alpha} + \pi \quad (\text{A20})$$

and the condition (A19) gives the following relations:

$$-\sin(2\tilde{\alpha})(1 + \cos\tilde{\beta}) = 2\sin\beta\sin\psi = R_{21}, \quad (\text{A21a})$$

$$-\cos(2\tilde{\alpha})(1 + \cos\tilde{\beta}) = \sin^2\beta + (1 + \cos^2\beta)\cos\psi = R_{11} + R_{22}, \quad (\text{A21b})$$

$$\cos\tilde{\beta} = \cos^2\beta + \sin^2\beta\cos\psi = R_{33}, \quad (\text{A21c})$$

$$\cos\tilde{\alpha}\sin\tilde{\beta} = \sin\beta\cos\beta(1 - \cos\psi) = R_{13}, \quad (\text{A21d})$$

$$\sin\tilde{\alpha}\sin\tilde{\beta} = -\sin\beta\sin\psi = R_{23}. \quad (\text{A21e})$$

From Eqs. (A21a) and (A21b), we derive the expression for the angle  $\tilde{\alpha}$  given in Eq. (31a) whereas the angle  $\tilde{\beta}$  is described by formulas (31b) and (31c) that can be easily obtained from Eqs. (A21c)–(A21e).

Our concluding remarks concern two special cases where either  $\sin \beta = 0$  or  $\cos \beta = 0$ . When  $\sin \beta = 0$  and  $\cos \beta = \pm 1$ , the operator (A11) describes rotations about the  $z$  axis by the angle  $\pm \psi$  and the angles  $\tilde{\alpha}$ ,  $\tilde{\beta}$  and  $\tilde{\gamma}$  are given by

$$\tilde{\beta} = 0, \quad \tilde{\alpha} + \tilde{\gamma} = \pm \psi. \quad (\text{A22})$$

At  $\cos \beta = 0$  and  $\sin \beta = \pm 1$ , the rotation axis is parallel to the  $x$  axis and we have

$$\tilde{\beta} = \pm \psi, \quad \tilde{\gamma} = -\tilde{\alpha} = \pi/2. \quad (\text{A23})$$

## APPENDIX B: QUANTIZED MICROWAVE FIELD AND POLYNOMIALLY DEFORMED ALGEBRAS

In the model with the Hamiltonian (5) the microwave field is treated as a classical field characterized by the  $c$ -number amplitude  $B$ . In this appendix we briefly discuss how this model can be extended to the case where, similar to the optical modes, the microwave field is quantized. In our analysis we employ the technique of polynomially deformed algebras to study applicability of the semiclassical approach.

For full quantum description of the modes, we begin with the Hamiltonian (3) rewritten as follows

$$H/\hbar = \Omega_{MW} N_b + \omega_{\text{opt}} N + \Omega J_z + \frac{2\gamma_0}{2S+1} (J_+ b + J_- b^\dagger), \quad (\text{B1})$$

where  $N_b = b^\dagger b$ , the operators  $J_z$  and  $J_\pm$  given by Eqs. (11)–(13) meet the commutation relations for generators of  $su(2)$  algebra (14), whereas the creation and annihilation operators of the microwave mode,  $b^\dagger$  and  $b$ , obey the commutation relation of the Heisenberg-Weyl algebra:  $[b, b^\dagger] = 1$ .

A set of operators that commute with the Hamiltonian (B1) contains three operators: (a) the operator of the total photon number for the optical modes  $N$  given in Eq. (11); (b) the Casimir operator of  $su(2)$  algebra  $J^2$  given by Eq. (15); and (c) the additional operator  $R = N_b + J_z$  related to the non-negative excitation number operator  $M = N_b + J_z + jI$ , where  $I$  is the identity operator and  $j$  is the angular momentum quantum number  $[j(j+1)$  is the eigenvalue of  $J^2$ ].

The Fock states for the model under consideration are represented by a direct product of the microwave and optical Fock states:  $|n_b\rangle_b \otimes |\psi\rangle_a$ , where  $n_b$  is the photon number of the microwave mode. The Fock space can be conveniently divided into subspaces  $\mathcal{F}_{n,m,j}$  classified by the quantum numbers  $m$ ,  $n$  and  $j$ , where  $m$ ,  $n$  and  $j(j+1)$  are the eigenvalues of the operators  $M$ ,  $N$  and  $J^2$ , respectively. The basis of  $\mathcal{F}_{n,m,j}$  can be formed from the eigenstates of the operator  $J_z$

$$|m, n, j, m_z\rangle = |m - m_z - j\rangle_b \otimes |n, j, m_z\rangle_a, \quad (\text{B2})$$

where  $-j \leq m_z \leq \min\{j, m - j\}$  is the azimuthal quantum number [the microwave photon number  $n_b = m - m_z - j$  is a non-negative integer] and  $J_z |m, n, j, m_z\rangle = m_z |m, n, j, m_z\rangle$ . Clearly, the quantum numbers  $m$  and  $j$  determine dimension of  $\mathcal{F}_{n,m,j}$ . At  $m \geq 2j$ , the quantum number  $m_z$  is ranged from  $-j$  to  $j$  and  $\dim \mathcal{F}_{n,m,j} = 2j + 1$ . In the opposite case with  $m < 2j$ , we have  $-j \leq m_z \leq m - j$  and  $\dim \mathcal{F}_{n,m,j} = m + 1$ .

In the subspace  $\mathcal{F}_{n,m,j}$ , the Hamiltonian (B1) is reduced to the following form:

$$H/\hbar = n \omega_{\text{opt}} + r\tilde{\Omega} - \omega M_0 + \frac{2\gamma_0}{2S+1} (M_+ + M_-), \quad (\text{B3})$$

where  $\tilde{\Omega} = (\Omega + \Omega_{MW})/2$ ,  $r = m - j$  is the eigenvalue of the operator  $R = N_b + J_z$  and the operators  $M_0$  and  $M_\pm$  are given by

$$M_- = bJ_+, \quad M_+ = b^\dagger J_-, \quad M_0 = \frac{N_b - J_z}{2}. \quad (\text{B4})$$

We can now closely follow the line of reasoning described in Ref. [53] and apply the methods of deformed (quantum) Lie algebras to solve the spectral problem for the Hamiltonian (B3). For this purpose, we note that the operators (B4) can be regarded as the generators of polynomial algebra of excitations (PAE). This algebra is generally defined through the algebraic relations:

$$[M_0, M_\pm] = \pm M_\pm, \quad M_+ M_- = p_\kappa(M_0), \quad (\text{B5})$$

where  $p_\kappa(q)$  is the structure polynomial of degree  $\kappa$  characterizing PAE of order  $\kappa$ . In our case, we have

$$M_+ M_- = N_b (J^2 - J_z^2 - J_z) = p_3(M_0), \quad (\text{B6})$$

$$p_3(q) = -(q - q_1)(q - q_2)(q - q_3), \quad (\text{B7})$$

where the roots of the polynomial  $p_3$  are given by

$$q_1 = \frac{j - m}{2}, \quad q_2 = \frac{m - 3j}{2}, \quad q_3 = \frac{m + j}{2} + 1. \quad (\text{B8})$$

The structure polynomial (B7) defines PAE of third order that will be denoted by  $\mathcal{M}_{m,j}$ . Since  $m \geq 0$ , the largest root is  $q_3$ , whereas relation between  $q_1$  and  $q_2$  depends on the values of  $m$  and  $j$ :  $q_1 > q_2$  at  $m < 2j$  and  $q_2 > q_1$  at  $m > 2j$ . When differences  $d_1 = q_3 - q_1 = m + 1$  and  $d_2 = q_3 - q_2 = 2j + 1$  are natural numbers,  $d_i \in \mathbb{N}$ , algebra  $\mathcal{M}_{m,j}$  is known to have finite-dimensional self-adjoint representations that correspond to the positive spectrum of  $p_3(M_0)$ .

When  $m > 2j$  [ $r > j$ ], the finite-dimensional irreducible representation of  $\mathcal{M}_{m,j}$  will be referred to as the *high-excitation zone*. Its dimension equals  $2j + 1$  and the corresponding spectrum of  $p_3(M_0)$  is ranged from  $q_2$  to  $q_3$ . In the opposite case with  $m < 2j$  [ $r < j$ ], the positive part of the spectrum lies in the interval  $[q_1, q_3]$  and the dimension of the representation — the so-called *low-excitation zone* — is equal to  $m + 1$ .

In the method of Ref. [53], the technique of polynomially deformed algebra is used to construct the transformations that map one polynomial algebra of operators onto another. More specifically, the representation of algebra  $\mathcal{M}_{m,j}$  with the generators  $\{M_0, M_+, M_-\}$  is related to a simpler algebra of second order with the generators  $\{S_0, S_+, S_-\}$  that meet the commutation relations of  $su(2)$  algebra (14) and its irreducible representation is characterized by the angular quantum number  $s$ . The number  $s$  is fixed by the requirement for two representations to be of the same dimension. Mathematical details on the method and a more accurate formulation of the key statements can be found in Ref. [53].

### A. High-excitation zone

First we consider the important case of the high-excitation zone, where  $s = j$  and the operators  $\{M_0, M_+, M_-\}$  are expressed in terms of  $\{S_0, S_+, S_-\}$  as follows [53]

$$M_0 = \frac{r}{2} - S_0, \quad M_+ = \sqrt{r - S_0} S_-, \quad (\text{B9})$$

$$M_- = [M_+]^\dagger = S_+ \sqrt{r - S_0},$$

where  $r = m - j$ . It is also not difficult to obtain the relations

$$S_0 = J_z, \quad S_+ = \frac{1}{\sqrt{N_b + 1}} a J_+, \quad S_- = J_- a^\dagger \frac{1}{\sqrt{N_b + 1}} \quad (\text{B10})$$

linking  $\{S_0, S_+, S_-\}$  and the operators that enter the Hamiltonian (B1).

We can now substitute relations (B9) into Eq. (B3) to obtain the Hamiltonian expressed in terms of the operators  $\{S_0, S_+, S_-\}$ . In the zero-order approximation, we have

$$M_0 = r/2 - S_0, \quad M_\pm \approx \sqrt{r + 1/2} S_\mp, \quad (\text{B11})$$

so that the approximate structure polynomial

$$p_2^{(s)}(M_0) = (r + 1/2) S_- S_+ = -(r + 1/2) (M_0 - q_2) (M_0 - q_3) \quad (\text{B12})$$

is quadratic. The corresponding zero-order Hamiltonian is given by

$$H_0^{(s)}/\hbar = n \omega_{\text{opt}} + r \Omega_{MW} + \omega S_0 + \frac{2\gamma_0}{2S + 1} \sqrt{r + 1/2} (S_+ + S_-). \quad (\text{B13})$$

A comparison between  $H_0^{(s)}$  and the quasienergy operator for the semiclassical model (22) shows that these operators are similar in algebraic structure. In particular, similar to formula (22), the quantum number  $j$  that determines the dimension of the representation does not enter the expression for  $H_0^{(s)}$ . So, when  $\gamma$  is replaced by  $\gamma_0 \sqrt{r + 1/2}$ , the spectra of these operators are identical up to the additive constant. We thus may conclude that the zero-order approximation for the high-excitation zone of the model with quantized microwave field reproduces the results of semiclassical approach. Note that the condition  $r > n_{\text{max}} S \equiv j_{\text{max}}$  ensures applicability of the semiclassical approximation for the Fock states of the optical modes whose total photon numbers are below  $n_{\text{max}}$ .

## B. Low-excitation zone

In conclusion, we briefly review the results for the low-excitation zone where  $m < 2j$ . The dimension of the representation is now equal to  $m + 1$ , so that  $s = m/2$ . The corresponding positive part of  $p_3(M_0)$  spectrum is ranged from  $q_1 = (j - m)/2$  to  $q_3 = (m + j)/2 + 1$  and relations linking  $\{M_0, M_+, M_-\}$  and  $\{S_0, S_+, S_-\}$  are given by

$$M_0 = \frac{j}{2} - S_0, \quad M_+ = \sqrt{2j - m/2 - S_0} S_-, \quad M_- = S_+ \sqrt{2j - m/2 - S_0}, \quad (\text{B14})$$

$$S_0 = \frac{m}{2} - N_b, \quad S_+ = J_+ \frac{1}{\sqrt{j - J_0}} a, \quad S_- = a^\dagger \frac{1}{\sqrt{j - J_0}} J_- \quad (\text{B15})$$

In the zero-order approximation, the operators (B14) are simplified as follows

$$M_0 = -S_0 + \frac{j}{2}, \quad M_\pm \approx \sqrt{(1 - m)/2 + 2j} S_\mp \quad (\text{B16})$$

and the approximate structure polynomial is given by

$$p_2^{(w)}(M_0) = -[(1 - m)/2 + 2j] (M_0 - q_1) (M_0 - q_3). \quad (\text{B17})$$

Finally, substituting relations (B16) into formula (B3) yields the expression for the zero-order Hamiltonian in the low-excitation zone

$$H_0^{(w)}/\hbar = n \omega_{\text{opt}} + \frac{m}{2} \Omega_{MW} + \frac{r}{2} \Omega + \omega S_0 + \frac{2\gamma_0}{2S + 1} \sqrt{(1 - m)/2 + 2j} (S_+ + S_-). \quad (\text{B18})$$

In contrast to the case of the high-excitation zone, the parameters of the Hamiltonian (B18) and the dimension of the representation both depend on the quantum numbers  $r$  and  $j$ . So, the semiclassical approximation breaks down in the low-excitation zone and quantum effects become essential for description of this regime even in the zero-order approximation.

## REFERENCES

1. M. Hayashi, S. Ishizaka, A. Kawachi, G. Kimura, and T. Ogawa, *Introduction to Quantum Information Science*, Graduate Texts in Physics (Springer, Berlin, 2015).
2. D. Bouwmeester, A. Ekert, and A. Zeilinger, eds., *The Physics of Quantum Information* (Springer, Berlin, 2000).
3. P. Kok and B. W. Lovett, *Introduction to Optical Quantum Information Processing* (Cambridge University Press, NY, 2010).
4. M. A. Nielsen and I. L. Chuang, *Quantum Computation and Quantum Information* (Cambridge University Press, NY, 2010), 10th ed.
5. A. Furusawa and P. van Loock, *Quantum Teleportation and Entanglement. A Hybrid Approach to Optical Quantum Information Processing* (Wiley-VCH, Berlin, 2011).
6. G. Cariolaro, *Quantum Communications, Signals and Communication Technology* (Springer, Berlin, 2015).
7. Y. Yamamoto, C. Santori, G. Solomon, J. Vuckovic, D. Fattal, E. Waks, and E. Diamanti, "Single photons for quantum information systems," *Progress in Informatics* pp. 5–37 (2005).
8. M. D. Eisaman, J. Fan, A. Migdall, and S. V. Polyakov, "Invited review article: Single-photon sources and detectors," *Review of Scientific Instruments* **82**, 071101 (2011).
9. C. Santori, D. Fattal, and Y. Yamamoto, *Single Photon Devices and Applications* (Wiley-VCH, Weinheim, 2010).
10. A. Migdall, S. V. Polyakov, J. Fan, and J. C. Bienfang, eds., *Single-Photon Generation and Detection: Physics and Applications*, vol. 45 of *Experimental Methods in the Physical Sciences* (Academic Press, NY, 2013).
11. M. Schiavon, G. Vallone, F. Ticozzi, and P. Villoresi, "Heralded single-photon sources for quantum-key-distribution applications," *Phys. Rev. A* **93**, 012331 (2016).
12. A. Muller, J. Breguet, and N. Gisin, "Experimental demonstration of quantum cryptography using polarized photons in optical fiber over more than 1 km," *Europhys. Lett.* **23**, 383–388 (1993).
13. A. Muller, H. Zbinden, and N. Gisin, "Underwater quantum coding," *Nature* **378**, 449 (1995).
14. A. Muller, H. Zbinden, and N. Gisin, "Quantum cryptography over 23 km in installed under-lake telecom fibre," *Europhys. Lett.* **33**, 335–339 (1996).
15. J.-M. M erolla, Y. Mazurenko, J.-P. Goedgebuer, and W. T. Rhodes, "Single-photon interference in sidebands of phase-modulated light for quantum cryptography," *Phys. Rev. Lett.* **82**, 1656–1659 (1999).
16. J.-M. M erolla, Y. Mazurenko, J.-P. Goedgebuer, L. Duraffourg, H. Porte, and W. T. Rhodes, "Quantum cryptographic device using single-photon phase modulation," *Phys. Rev. A* **60**, 1899–1905 (1999).
17. A. K. Ekert, "Quantum cryptography based on Bell's theorem," *Phys. Rev. Lett.* **67**, 661–663 (1991).
18. W. Tittel, J. Brendel, H. Zbinden, and N. Gisin, "Quantum cryptography using entangled photons in energy-time Bell states," *Phys. Rev. Lett.* **84**, 4737–4740 (2000).
19. G. Ribordy, J. Brendel, J.-D. Gautier, N. Gisin, and H. Zbinden, "Long-distance entanglement-based quantum key distribution," *Phys. Rev. A* **63**, 012309 (2000).

20. N. Gisin, G. Ribordy, W. Tittel, and H. Zbinden, "Quantum cryptography," *Rev. Mod. Phys.* **74**, 145–195 (2002).
21. U. L. Andersen, G. Leuchs, and C. Silberhorn, "Continuous-variable quantum information processing," *Laser & Photonics Reviews* **4**, 337–354 (2010).
22. C. Weedbrook, S. Pirandola, R. García-Patrón, N. J. Cerf, T. C. Ralph, J. H. Shapiro, and S. Lloyd, "Gaussian quantum information," *Rev. Mod. Phys.* **84**, 621–669 (2012).
23. M. Bloch, S. W. McLaughlin, J.-M. Merolla, and F. Patois, "Frequency-coded quantum key distribution," *Opt. Lett.* **32**, 301–303 (2007).
24. P. Kolchin, C. Belthangady, S. Du, G. Y. Yin, and S. E. Harris, "Electro-optic modulation of single photons," *Phys. Rev. Lett.* **101**, 103601 (2008).
25. S. E. Harris, "Nonlocal modulation of entangled photons," *Phys. Rev. A* **78**, 021807 (2008).
26. S. Sensarn, G. Y. Yin, and S. E. Harris, "Observation of nonlocal modulation with entangled photons," *Phys. Rev. Lett.* **103**, 163601 (2009).
27. L. Olislager, J. Cussey, A. T. Nguyen, P. Emplit, S. Massar, J.-M. Merolla, and K. P. Huy, "Frequency-bin entangled photons," *Phys. Rev. A* **82**, 013804 (2010).
28. A. V. Gleim, V. I. Egorov, Y. V. Nazarov, S. V. Smirnov, V. V. Chistyakov, O. I. Bannik, A. A. Anisimov, S. M. Kynev, A. E. Ivanova, R. J. Collins, S. A. Kozlov, and G. S. Buller, "Secure polarization-independent subcarrier quantum key distribution in optical fiber channel using BB84 protocol with a strong reference," *Opt. Express* **24**, 254859 (2016).
29. J.-M. Liu, *Photonic Devices* (Oxford University Press, New York, 2005).
30. A. Yariv and P. Yeh, *Photonics: Optical Electronics in Modern Communications* (Oxford University Press, New York, 2007), 6th ed.
31. L. M. Blinov and V. G. Chigrinov, *Electrooptic effects in liquid crystal materials* (Springer-Verlag, New York, 1994).
32. S. P. Kotova, S. A. Samagin, E. P. Pozhidaev, and A. D. Kiselev, "Light modulation in planar aligned short-pitch deformed-helix ferroelectric liquid crystals," *Phys. Rev. E* **92**, 062502 (2015).
33. A. D. Kiselev and V. G. Chigrinov, "Optics of short-pitch deformed-helix ferroelectric liquid crystals: Symmetries, exceptional points, and polarization-resolved angular patterns," *Phys. Rev. E* **90**, 042504 (2014).
34. E. P. Pozhidaev, A. K. Srivastava, A. D. Kiselev, V. G. Chigrinov, V. V. Vashchenko, A. V. Krivoshey, M. V. Minchenko, and H.-S. Kwok, "Enhanced orientational Kerr effect in vertically aligned deformed helix ferroelectric liquid crystals," *Optics Letters* **39**, 2900–2903 (2014).
35. E. P. Pozhidaev, A. D. Kiselev, A. K. Srivastava, V. G. Chigrinov, H.-S. Kwok, and M. V. Minchenko, "Orientational Kerr effect and phase modulation of light in deformed-helix ferroelectric liquid crystals with subwavelength pitch," *Phys. Rev. E* **87**, 052502 (2013).
36. M. Tsang, J. H. Shapiro, and S. Lloyd, "Quantum theory of optical temporal phase and instantaneous frequency," *Phys. Rev. A* **78**, 053820 (2008).
37. M. Tsang, J. H. Shapiro, and S. Lloyd, "Quantum theory of optical temporal phase and instantaneous frequency. II. Continuous-time limit and state-variable approach to phase-locked loop design," *Phys. Rev. A* **79**, 053843 (2009).
38. P. A. M. Dirac, "The quantum theory of the emission and absorption of radiation," *Proc. R. Soc. Lond. A* **114**, 243–265 (1927).
39. S. M. Barnett and J. A. Vaccaro, eds., *The Quantum Phase Operator: A Review*, Series in Optics and Optoelectronics (Taylor & Francis, NY, 2007).
40. J. Capmany and C. R. Fernández-Pousa, "Quantum model for electro-optical phase modulation," *J. Opt. Soc. Am. B* **27**, A119–A129 (2010).
41. J. Capmany and C. Fernández-Pousa, "Quantum modelling of electro-optic modulators," *Laser & Photonics Reviews* **5**, 750–772 (2011).
42. W. H. Louisell, A. Yariv, and A. E. Siegman, "Quantum fluctuations and noise in parametric processes. I," *Phys. Rev.* **124**, 1646–1654 (1961).
43. W. She and W. Lee, "Wave coupling theory of linear electrooptic effect," *Optics Communications* **195**, 303–311 (2001).
44. D. Wu, H. Chen, W. She, and W. Lee, "Wave coupling theory of the linear electro-optic effect in a linear absorbent medium," *J. Opt. Soc. Am. B* **22**, 2366–2371 (2005).
45. P. Kumar and A. Prabhakar, "Evolution of Quantum States in an Electro-Optic Phase Modulator," *IEEE Journal of Quantum Electronics* **45**, 149–156 (2009).
46. D. A. Cohen and A. F. J. Levy, "Microphotonic components for a mm-wave receiver," *Solid State Electronics* **45**, 495–505 (2001).
47. V. S. Ilchenko, A. A. Savchenkov, A. B. Matsko, and L. Maleki, "Whispering-gallery-mode electro-optic modulator and photonic microwave receiver," *J. Opt. Soc. Am. B* **20**, 333–342 (2003).
48. A. A. Savchenkov, W. Liang, A. B. Matsko, V. S. Ilchenko, D. Seidel, and L. Maleki, "Tunable optical single-sideband modulator with complete sideband suppression," *Opt. Lett.* **34**, 1300–1302 (2009).
49. A. Rasoloniaina, V. Huet, T. K. N. Nguyễn, E. L. Cren, M. Mortier, L. Michely, Y. Dumeige, and P. Féron, "Controlling the coupling properties of active ultrahigh-Q WGM microcavities from undercoupling to selective amplification," *Scientific Reports* **4**, 4023 (2014).
50. A. B. Matsko, A. A. Savchenkov, V. S. Ilchenko, D. Seidel, and L. Maleki, "On fundamental quantum noises of whispering gallery mode electro-optic modulators," *Opt. Express* **15**, 17401–17409 (2007).
51. A. Savchenkov, A. Matsko, W. Liang, V. Ilchenko, D. Seidel, and L. Maleki, "Single-sideband electro-optical modulator and tunable microwave photonic receiver," *IEEE Transactions on Microwave Theory and Techniques* **58**, 3167–3174 (2010).
52. M. Tsang, "Cavity quantum electro-optics," *Phys. Rev. A* **81**, 063837 (2010).
53. I. P. Vadeiko, G. P. Miroshnichenko, A. V. Rybin, and J. Timonen, "Algebraic approach to the Tavis-Cummings problem," *Phys. Rev. A* **67**, 053808 (2003).
54. F. Dell'Anno, S. De Siena, and F. Illuminati, "Multiphoton quantum optics and quantum state engineering," *Physics Reports* **428**, 53–168 (2006).
55. J.-M. Mérolla, Y. Mazurenko, J.-P. Goedgebuer, H. Porte, and W. T. Rhodes, "Phase-modulation transmission system for quantum cryptography," *Opt. Lett.* **24**, 104–106 (1999).
56. A. Ortigosa-Blanch and J. Capmany, "Subcarrier multiplexing optical quantum key distribution," *Phys. Rev. A* **73**, 024305 (2006).
57. J. A. Armstrong, N. Bloembergen, J. Ducuing, and P. S. Pershan, "Interactions between light waves in a nonlinear dielectric," *Phys. Rev.* **127**, 1918–1939 (1962).
58. J. P. Gordon, W. H. Louisell, and L. R. Walker, "Quantum fluctuations and noise in parametric processes. II," *Phys. Rev.* **129**, 481–485 (1963).
59. L. S. Brown and L. J. Carson, "Quantum-mechanical parametric amplification," *Phys. Rev. A* **20**, 2486–2497 (1979).
60. V. V. Dodonov, A. B. Klimov, and D. E. Nikonov, "Quantum phenomena in nonstationary media," *Phys. Rev. A* **47**, 4422–4429 (1993).
61. L. C. Biedenharn and J. D. Louck, *Angular Momentum in Quantum Physics: Theory and Application*, vol. 8 of *Encyclopedia of Mathematics and its Applications* (Addison-Wesley, Reading, Massachusetts, 1981).
62. D. A. Varshalovich, A. N. Moskalev, and V. K. Khersonskii, *Quantum theory of angular momentum: Irreducible tensors, spherical harmonics, vector coupling coefficients, 3nj symbols* (World Scientific Publishing Co., Singapore, 1988).
63. L. Olislager, I. Mbodji, E. Woodhead, J. Cussey, L. Furfaro, P. Emplit, S. Massar, K. P. Huy, and J.-M. Merolla, "Implementing two-photon interference in the frequency domain with electro-optic phase modulators," *New Journal of Physics* **14**, 043015 (2012).
64. H. Carmichael, *An Open Systems Approach to Quantum Optics* (Springer, Berlin, Heidelberg, 1993).
65. L. Mandel and E. Wolf, *Optical Coherence and Quantum Optics* (Cambridge University Press, Cambridge, 1995).
66. M. Abramowitz and I. A. Stegun, eds., *Handbook of Mathematical Functions* (Dover, New York, 1972).
67. G. Szegő, *Orthogonal Polynomials* (American Mathematical Society, Providence, Rhode Island, 1975), 4th ed.
68. M. Aspelmeyer, T. J. Kippenberg, and F. Marquardt, eds., *Cavity Optomechanics: Nano- and Micromechanical Resonators Interacting with Light*, Quantum Science and Technology (Springer, Berlin, Heidelberg, 2014).
69. M. Aspelmeyer, T. J. Kippenberg, and F. Marquardt, "Cavity optomechanics," *Rev. Mod. Phys.* **86**, 1391–1452 (2014).